Journal of the Serbian Chemical Society
JSCS@tmf.bg.ac.rs • www.shd.org.rs/JSCS
J. Serb. Chem. Soc. *89* (11) 1447–1460 (2024)
JSCS–5799
Original scientific paper
Published 3 December, 2024

Identification of musk compounds as inhibitors of the main SARS-CoV-2 protease by molecular docking and molecular dynamics studies

ASSIA BELHASSAN[1], GUILLERMO SALGADO[2], LUIS HUMBERTO MENDOZA-HUIZAR[3]*, HANANE ZAKI[4], SAMIR CHTITA[5], TAHAR LAKHLIFI[1], MOHAMMED BOUACHRINE[1,4], LORENA GERLI CANDIA[6] and WILSON CARDONA[7]

[1]Molecular Chemistry and Natural Substances Laboratory, Faculty of Science, Moulay Ismail University of Meknes, Morocco, [2]Facultad de Ciencias Químicas. Investigador Extramural, Universidad de Concepción, Concepción, Chile, [3]Autonomous University of Hidalgo State. Academic Area of Chemistry. Mineral de la Reforma, Hidalgo. México, [4]EST Khenifra, Sultan Moulay Sliman University, Benimellal, Morocco, [5]Laboratory of Analytical and Molecular Chemistry, Department of Chemistry, Faculty of Sciences Ben M'Sik, Hassan II University of Casablanca, Casablanca, Morocco, [6]Departamento de Química Ambiental, Facultad de Ciencias, Universidad Católica de la Santísima Concepción, Concepción, Chile and [7]Facultad de Medicina y Ciencia, Universidad San Sebastián, Puerto Montt, Chile

(Received 25 November, revised 22 December 2023, accepted 19 February 2024)

Abstract: As new drug development is a long process, reuse of bioactives may be the answer to new epidemics; thus, screening existing bioactive compounds against a new SARS-CoV-2 infection is an important task. With this in mind, we have systematically screened potential odorant molecules in the treatment of this infection based on the affinity of the selected odorant compounds on the studied enzyme and the sequence identity of their target proteins (olfactory receptors) to the same enzyme (the main protease of SARS-CoV-2). A total of 12 musk odorant compounds were subjected to a molecular docking and molecular dynamics study to predict their impact against the main protease of SARS-CoV-2. In this study, we have identified two musk-scented compounds (androstenol and vulcanolide) that have good binding energy at the major protease binding site of SARS-CoV-2. However, the *RMSD* values recorded during dynamic simulation show that vulcanolide exhibits high stability of the protein–ligand complex compared to androstenol. The perspectives of this work are as follows: *in vitro*, *in vivo* and clinical trials to verify the computational findings.

Keywords: coronavirus; musk-smelling compounds; olfactory receptors; molecular docking; molecular dynamics.

* Corresponding author. E-mail: hhuizar@uaeh.edu.mx
https://doi.org/10.2298/JSC231125012B

INTRODUCTION

A new form of infection, the coronavirus caused by the SARS-CoV-2 virus, has spread rapidly around the world,[1–5] and continues to kill thousands of people every day. This new form of coronavirus occurred in December 2019 in Wuhan, China,[6] and to date no effective treatment against SARS-CoV-2 virus infection has been reported.[7,8] The possible treatment of coronaviruses can be carried out in two different ways: the first by strengthening the human immune system, and the second by attacking the coronavirus itself.[2] This virus is a member of the beta-coronavirus family.[9] It infects cells by binding to ACE2 by its spike glycoprotein (S). In order to complete the entry into the cell, the protease enzyme must prime the spike glycoprotein; this protease is called TMPRSS2. In fact, the activation of TMPRSS2 as a protease is needed to attach the spike protein of the virus to its human cellular ligand. The viral genome is transcribed and then translated after the virus enters the host cell and uncoats. Therefore, targeting and disturbing the operation of one or many of those enzymes involved in viral replication, transcription, or translation can be effective in stopping the emergency of this pandemic.[2] Here, it is important to mention that the structure-biology study of coronavirus (SARS-CoV-2) proteins is still at an early stage. The crystal structure of the main protease, also named 3CLpro or 3-chymotrypsin-like protease,[2] has many PDB structures (PDB code: 6LU7, 6M03, 6W4B, 6Y84, 6YB7, 5R7Y, 5R7Z, 5R80, 5R81, 6W63, 6M3M…).[10] However, in this study, we are interested in the crystal structure of 3CLpro (PDB code: 6LU7) because the protease activity that is responsible for polyprotein cleavage is present in this enzyme (nsp5 protein).[11] This crystallographic structure is encoded within the viral genome in complex with the N3 inhibitor.[12] Here it is worth mentioning that the reuse of bioactive compounds can be a good option in the face of the outbreak of unexpected infectious diseases due to the long production time of new drugs.[3,13] For example, the effect of chloroquine and hydroxychloroquine in the treatment of COVID-19 has been evaluated in many research papers,[3,14–16] and in fact, these two drugs are used worldwide for the treatment of COVID-19 disease.[17,18] Therefore, there is an urgent task to discover novel bioactives with new methodologies to combat COVID-19 disease; and consequently, the challenge is to detect chemical compounds with inhibitory effects on the SARS-CoV-2 main protease virus. Specifically, in the event of a pulmonary infection, volatile compounds are very useful since the respiratory system will positively support therapies of this kind.[19] Thus, the chemical constituents present in aromatic plants have the potential to inhibit viral infections.[19–23] Musk-smelling compounds are well known as a very odorous material, which is the secretion of the musk-carrying Chevrotin.[24] These musk-smelling compounds are able to activate the human musk receptors OR5AN1 and OR1A1, and they could activate other kinds of receptors if they have homology. In this sense, two receptors have homology when

their structures share a significant sequence similarity (a percentage of identity greater than 40 % is considered to be a sign of homology unless the sequences are of low complexity). Although a complete lack of similarity does not mean an absence of homology, Moreover, the significant increase in the number of known 3D structures has made it clear that in many cases, two sequences with sequence identities of the order from 20 to 40 % adopt similar folds and may have similar functions.[25] It is therefore important to look for possible structural analogies and determine if these can correspond to common biological functions.[25]. To the best of our knowledge and based on exhaustive bibliographic research, the homology between the olfactory receptors (OR5AN1, OR1A1) and the 6LU7 has not been analyzed. Thus, in this paper, the goal is to evaluate the potential efficiency of 12 Musk-smelling compounds against novel coronaviruses by searching for the sequence identity of their biological targets (olfactory receptors) with the 6LU7 and comparing the affinity and stability of these molecules at the binding site by molecular docking and molecular dynamic methods, respectively.[26,27]

EXPERIMENTAL

Data set

In this study, we have chosen 12 musk-smelling compounds based on the fact that their targets have a good sequence identity with 6LU7. These compounds are (3*R*)-3-methylcyclopentadecan-1-one (*R*-muscone), 1,4-dioxacycloheptadecane-5,17-dione (ethylene brassylate), 5*α*-androst-16-en-3*α*-ol (androstenol), (9*Z*)-cycloheptadec-9-en-1-one (civeton), (8*Z*)-1-oxacycloheptadec-8-en-2-one (ambrettolide), (6*R*,7*R*)-3,5,5,6,7,8,8-heptamethyl-5,6,7,8-etrahydronaphthalene-2-carbaldehyde (vulcanolide), as-hydryndacene-1-ol (hydrindacene), 1-(3,5,5,6,8,8-hexamethyl-6,7-dihydronaphthalen-2-yl)ethenone (fixolide), 1-tert-butyl-3,5-dimethyl-2,4,6-trinitrobenzene (musk xylene), 1,1,3,3,5-pentamethyl-4,6-dinitroindane (moskene), 1-(4-tert-butyl-2,6-dimethyl-3,5-dinitrophenyl)ethan-1-one (musk ketone) and 4-tert-butyl-3-methoxy-2,6-dinitrotoluene (musk ambrette). Fig. 1 shows the chemical structure of these compounds.

Sequence identity

The comparison between the sequence of SARS-CoV-2 main protease (PDB code 6LU7, chain A) and the selected olfactory receptors was carried out using the Swiss-Model modelling server (http://swissmodel.expasy.org).[28] To determine the sequence identity between SARS--CoV-2 main protease and these targets,[29-32] these targets are selected according to their sequence identity (ID) with SARS-CoV-2 main protease. All studied compounds were obtained from chemical structure databases such as ChemSpider (An Online Chemical Information Resource).[33]

Molecular docking

We performed a molecular docking study of 12 odorant molecules (Fig. 1). The ligands (12 Musk-smelling compounds) of selected olfactory receptors (ORs) are indicated in the literature.[34] The computational study was carried out with two programs; Autodock vina and Autodock tools 1.5.6.[35] The ligands and macromolecule preparation was carried out by Discovery Studio 2016 program,[36] the structure of SARS-CoV-2 main protease (PDB code 6LU7, chain A)[37] was imported to detect the binding site of this enzyme.[27] The center coordinates of

the binding site are: x = –10.782, y = 15.787 and z = 71.277,[38] and the grid size was set at 20×20×20 *xyz* points with a grid spacing of 1 Å using N3 (co-crystallized ligand) as the center for docking to determinate the accurate size.[38]

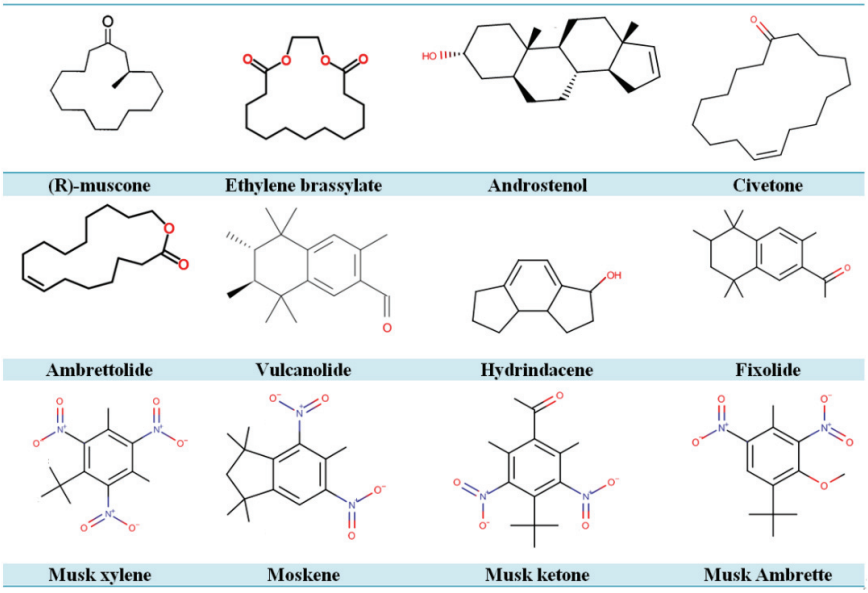

Fig. 1. Musk-smelling compounds used in this study (their targets are human olfactory receptors O5AN1 and OR1A1).

Molecular dynamic (MD) simulation

In order to validate whether the orientation and interaction energy in the active pocket predicted by molecular docking correspond to stable and biologically relevant binding, we performed a 100 ns molecular dynamics study of androstenol-3CLpro and vulcanolide-3CLpro. The water was modelled using the TIP3P equation and placed in the octahedron center for a 100 ns MD simulation. Molecular dynamics calculation and visualization were performed using the programs GROMACS[39] and USCF-Chimera,[40] respectively. Prior to the MD simulation, an energy minimization process was performed and then equilibration process was conducted in two phases. The first one was conducted under an NVT ensemble (constant number of particles, volume, and temperature) and in the next step, the equilibrium of pressure was conducted under an NPT ensemble (isothermal-isobaric ensemble) for 1 ns. Then a MD for 100 ns was conducted to analyze the stability of the protein–ligand complex.

Molecular electrostatic potential (MEP)

It is widely recognized that MEP is capable of helping determine a molecule's relative polarity, which highlights a variety of interactions, including those involving chemical reactivity, hydrogen bonds and compounds that are biologically active.[41,42] In this work, the basis set 6-31G(d) and the hybrid functional B3LYP[43,44] have been used to calculate MEP using the Gaussian 09 package[45] and GaussView 5.08.[46]

RESULTS AND DISCUSSION

Molecular docking

The top-scoring pose of each odorant molecule is presented according to the best energy of interaction in the binding pocket of the SARS-CoV-2 main protease (Table I), and their targets (olfactory receptors (ORs)) present a good ID with the SARS-CoV-2 main protease: human olfactory receptor O5AN1 has the code UniProtKB: Q8NGI8 and *ID* = 31.08 % with the SARS-CoV-2 main protease; human olfactory receptor OR1A1 has the code UniProtKB: Q9P1Q5 and *ID* = = 35.29 % with SARS-CoV-2 main protease.

This methodology was performed to find potential drugs for the studied enzyme and the results are presented in Table I.

TABLE I. Binding free energies, binding equilibrium constant and dissociation equilibrium constant of Musk-smelling compounds in the binding site of the studied enzyme, and information about their protein targets (ORs)

N°	Potential drug	Binding free energies with 6LU7, kJ mol^{-1}	Binding equilibrium constant, $K_B \times 10^{-4}$ / M^{-1}	Dissociation equilibrium constant, $K_D \times 10^{5}$ / M^{-1}	Target and sequence identity with 6LU7
1	Androstenol	–28.0	8.1	1.2	Human olfactory receptor O5AN1 code UniProtKB: Q8NGI8 ID = 31.08 %
2	Vulcanolide	–25.9	3.5	2.9	
3	Fixolide	–25.5	3.0	3.4	
4	Civetone	–25.5	3.0	3.4	
5	Ambrettolide	–25.5	3.0	3.4	
6	Ethylene brassylate	–25.5	3.0	3.4	
7	(*R*)-Muscone	–25.1	2.5	4.0	Human olfactory receptor OR1A1 code UniProtKB: Q9P1Q5 *ID* = 35.29 %
8	Moskene	–25.1	2.5	4.0	
9	Musk ambrette	–24.3	1.8	5.5	
10	Hydrindacene	–24.3	1.8	5.5	
11	Musk xylene	–23.8	1.5	6.7	
12	Musk ketone	–23.0	1.1	9.3	

Here, it is important to mention that in a docking study, the scoring functions evaluate the binding affinity, which is directly related to the Gibbs energy change of binding ($\Delta_B G^0$),[47] and this energy is the driving force for the acceptor–receptor binding process.[48,49] From this $\Delta_B G^0$ it is possible to evaluate the binding equilibrium constant (K_B) through the Eq. (1):[50]

$$K_B = e^{-\frac{\Delta_B G^0}{RT}} \quad (1)$$

In addition, the binding strength of a ligand can also be evaluated by the thermodynamic dissociation constant, K_D, which measures the strength of binding of the ligand to the protein.[51] Thus, K_D is the equilibrium constant of the

ligand–protein complex dissociation reaction in the free protein and the ligand and is defined as:[51]

$$K_D = \frac{1}{K_B} \quad (2)$$

In Table I, the values of K_B and K_D for the musk compounds docked to 6LU7 are reported. Note that the results indicate that androstenol and vulcanoide interacted the best with both studied receptors, with binding free energies equal to –28 and –25.9 kJ mol^{-1}, respectively. Also, the ligands androstenol and vulcanolide represent the highest binding equilibrium constant values, indicating a high binding affinity between 6LU7 and these ligands.[50] For androstenol and vulcanoide, the K_D values are 0.012 and 2.9 M^{-1}, respectively. These K_D values are lower than those found for the binding of glycans to the SARS-CoV-2 spike protein,[52] suggesting a high affinity of androstenol and vulcanoide to 6LU7. Thus, it is clear that these two musk-smelling compounds present the best energies of interaction with the SARS-CoV-2 main protease, see Table I. We can also observe that their target has a good ID with the SARS-CoV-2 main protease. Based on the effect that structural homology is sometimes linked to functional homology,[25] two sequences with sequence identities of the order from 20 to 40 % adopt similar folds and may have similar functions. Thus, it is important to look for the selected musk-smelling compounds (androstenol and vulcanolide); these volatile molecules are very useful since the respiratory system will positively support therapies of this kind. The two selected molecules could have good inhibitory effects on the SARS-CoV-2 main protease.[30]

The interaction results of androstenol in the binding site of the SARS-CoV-2 main protease (Fig. 2) show hydrogen bond interaction and a carbon-hydrogen bond with His163 and Met165, respectively.

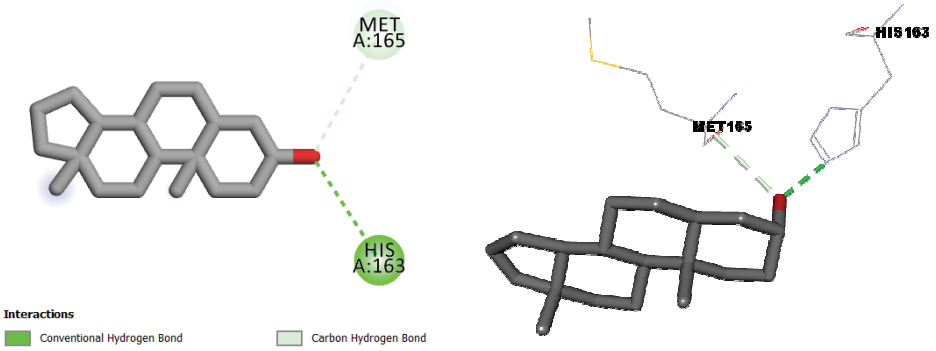

Fig. 2. Interactions between androstenol and the SARS-CoV-2 main protease.

The interaction results of vulcanolide in the binding site of the SARS-CoV-2 main protease (Fig. 3) show alkyl and π-alkyl interactions with Met49, Cys145, and His41.

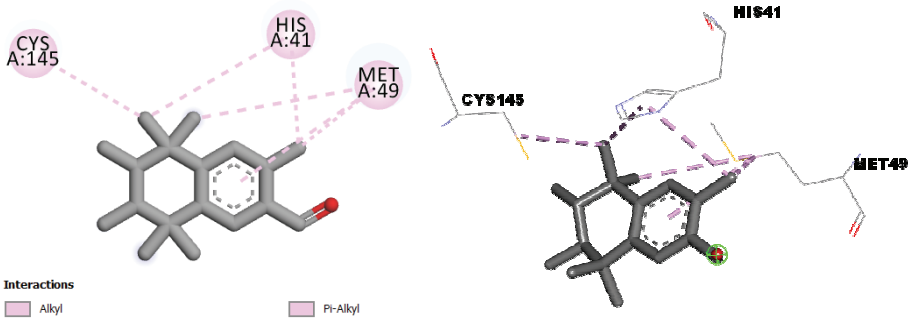

Fig. 3. Interactions between vulcanolide and the SARS-CoV-2 main protease.

Molecular dynamic (MD) simulation

The complex androstenol-3CLpro was unstable and after 1 ns of MD simulation androstenol compound get out from the pocket site of 3CLpro (not shown). The last one is probably due to the fewer interactions between this molecule and the pocket site (see Fig. 2). In the case of the vulcanoide-3CL procomplex, a MD simulation of 100 ns shows the complex is stable. In Fig. 4, the potential energy behavior of the complex is depicted during the MD simulation. It may be seen that the potential energy of the protein-ligand complex lies in the range from -2.86×10^5 to -2.88×10^5 kJ mol^{-1} and reaches a constant level after approx. 10 ns.

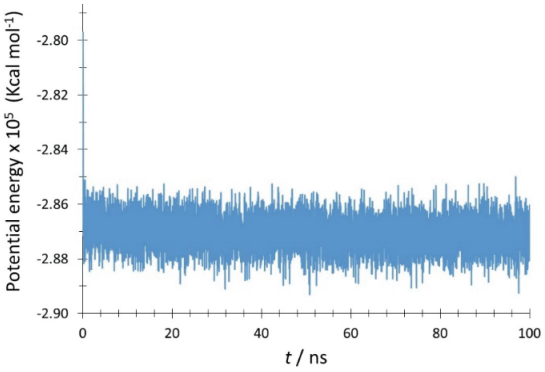

Fig. 4. Variation of the potential energy *vs*. simulation time.

Also, we mapped the interactions of vulcanolide with the closer residues in the pocket site of 3CLpro, and they are summarized in Table II. Note that at 0 ns, the main interactions are with the residues Cys145, His41 and Met49. However, at 10 ns, the main interactions are with His41, Met49 and Met165, suggesting a

modification of the vulcanolide position in the pocket site. At 40 ns, the ligand modifies its position again, but from 50 ns, in all cases, the ligand keeps strong interactions with His41, Met49 and Met165 to the end of the simulation, suggesting that a stable conformation was reached.

TABLE II. Interactions of vulcanolide with 3CLpro during the MD simulation

t / ns	Interacting residue						
0	Cis145		His41	Met49			
10			His41	Met49	Met165		
20			His41	Met49	Met165		
30			His41	Met49	Met165		
40		Cys44	His41		Met165		
50			His41	Met49	Met165	Leu167	
60			His41	Met49	Met165		Gln189
70			His41	Met49	Met165		
80		Cys44	His41	Met49	Met165		
90			His41	Met49	Met165		
100			His41	Met49	Met165		

In Fig. 5, the variation of the distances of vulcanolide to the residues His41, Met49 and Met165 is depicted. Note that after 45 ns, the separation distance between His41, Met49 and Met165 drops drastically from 6 to 3 Å, and the distances are kept at the end of the simulation, indicating that a stable configuration is reached.

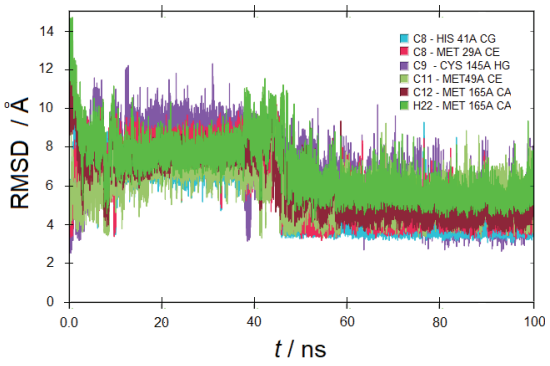

Fig. 5. *RMSD* of the characteristic distances between the ligand (purple) and the enzyme *vs*. simulation time.

Also, the *RMSD* plots of the drug and the complex were obtained separately, and they are depicted in Fig. 6. Note that vulcanolide equilibrates rather quickly than the protein, but the complex equilibrates until after 60 ns, and after this time, the complex is stable.

Also, the coulomb interaction energy was analyzed (Fig. 7). At the end of the simulation, this energy shows a value of –401 kJ mol^{-1}, suggesting a strong interaction between the protein and the ligand.

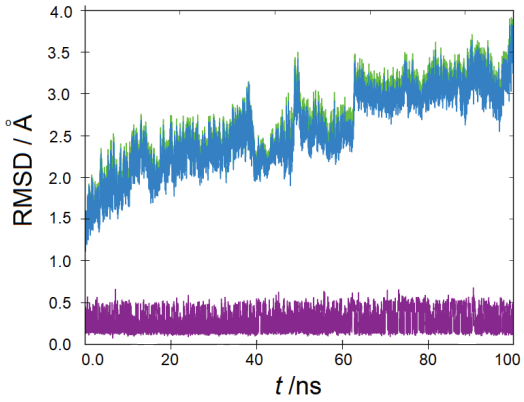

Fig. 6. *RMSD* of the ligand (purple), enzyme (green) and the ligand–enzyme complex (blue) *vs*. simulation time.

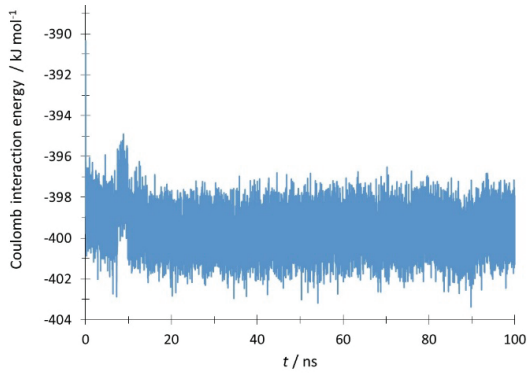

Fig. 7. Variation of the Coulomb interaction energy during the simulation.

Molecular electrostatic potential (MEP)

Fig. 8 shows the MEP for vulcanolide. The red color indicates the existence of a higher electron density site, while the blue color is associated with charge deficiency and the presence of a maximum positive charge, and these sites are primarily nucleophilic. If one compares the interactions observed in Fig. 3 between vulcanolide and SARS-CoV-2, note that vulcanolide is interacting with 3CLpro through its nucleophilic sites.

CONCLUSION

In this study, we have identified potential drugs that could have an effect on the studied enzyme. This research will provide new principal musk-smelling compounds that could have a good effect against SARS-CoV-2 main protease because of their affinity energy and stability in the binding site of the studied enzyme and their good sequence identity (*ID*) with the same enzyme (SARS--CoV-2 main protease). Androstenol and vulcanolide have the best energies of interaction with the SARS-CoV-2 main protease. We can also observe that their selected target has a good ID with the SARS-CoV-2 main protease. Based on the

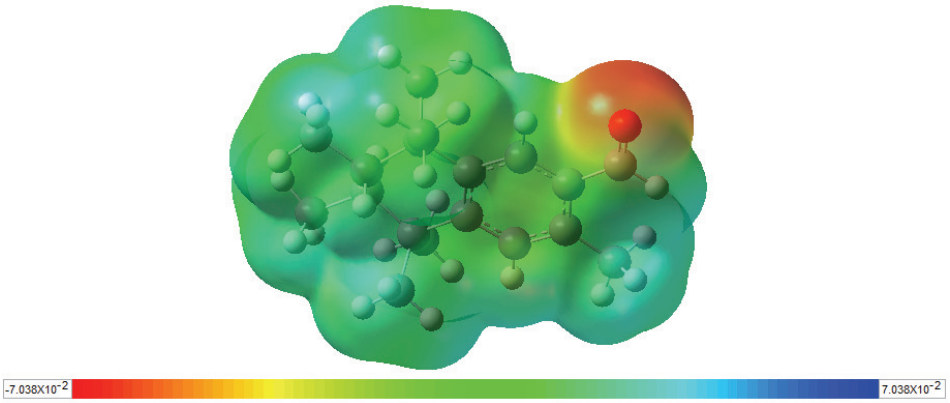

Fig. 8. Maps of molecular electrostatic potential obtained at the B3LYP/6-31G(d) level of theory onto a density isosurface of 0.002 e/u.a.^{3}, for vulcanolide molecule.

fact that structural homology is sometimes linked to functional homology, it is important to look for the selected compounds that could have good inhibitory effects on the SARS-CoV-2 main protease. The *RMSD* values recorded during the simulation (for drug vulcanolide) and fairly low potential energy of -2.88×10^5 kJ mol^{-1} show the high stability of the protein ligand complex and the likeliness of the vulcanolide molecule to be a drug-like candidate. Thus, the evaluation of the activity, *in vitro* and *in vivo*, of vulcanolide against COVID-19 could be interesting.

Acknowledgements. The authors would like to thank the Research Department of the Universidad Católica de la Santísima Concepción for its support through the DIREG 03/2020 project. L. H. Mendoza-Huizar thankfully acknowledges the computer resources, technical expertise and support provided by the Laboratorio Nacional de Supercómputo del Sureste de México, Consejo Nacional de Ciencia y Tecnología (CONACYT) member of the network of national laboratories through the project No. 202203072N and to the Universidad Autónoma del Estado de Hidalgo.

ИЗВОД

ИДЕНТИФИКАЦИЈА МОШУСНИХ ЈЕДИЊЕЊА КАО ИНХИБИТОРА ГЛАВНЕ SARS-COV-2 ПРОТЕАЗЕ, СТУДИЈАМА МОЛЕКУЛСКОГ ДОКИНГА И МОЛЕКУЛСКЕ ДИНАМИКЕ

ASSIA BELHASSAN[1], GUILLERMO SALGADO[2], LUIS HUMBERTO MENDOZA-HUIZAR[3],HANANE ZAKI[4], SAMIR CHTITA[5], TAHAR LAKHLIFI[1], MOHAMMED BOUACHRINE[1,4], LORENA GERLI CANDIA[6] и WILSON CARDONA[7]

[1]Molecular Chemistry and Natural Substances Laboratory, Faculty of Science, Moulay Ismail University of Meknes, Morocco, [2]Facultad de Ciencias Químicas. Investigador Extramural, Universidad de Concepción, Concepción, Chile, [3]Autonomous University of Hidalgo State. Academic Area of Chemistry. Mineral de la Reforma, Hidalgo. México, [4]EST Khenifra, Sultan Moulay Sliman University, Benimellal, Morocco, [5]Laboratory of Analytical and Molecular Chemistry, Department of Chemistry, Faculty of Sciences Ben M'Sik, Hassan II University of Casablanca, Casablanca, Morocco, [6]Departamento de Química Ambiental, Facultad de Ciencias, Universidad Católica de la Santísima Concepción, Concepción, Chile и [7]Facultad de Ciencias Exactas, Departamento de Química. Universidad Andrés Bello. Concepción, Chile

Пошто је развој нових лекова дуготрајан процес, поновна употреба биоактивних супстанци би могла бити одговор на нове епидемије; тако је скрининг постојећих биоактивних једињења према новој SARS-CoV-2 инфекцији важан задатак. Са тиме на уму, ми смо систематски прегледали потенцијалне мирисне молекуле за третирање ове инфекције на бази афинитета одабраних мирисних једињења према проучаваном ензиму и идентичност секвенце њихових циљних протеина (олфакторни рецептори) према истом ензиму (главна протеаза SARS-CoV-2). Укупно је 12 мошусних мирисних једињења подвргнуто студији докинга и молекулске динамике да би предвидели њихов утицај на главну протеазу SARS-CoV-2. У овој студији идентификовали смо два једињења мошусног мириса (андростенол и вулканолид) која имају добру енергију везивања на везивно место главне протеазе SARS-CoV-2. Међутим, *RMSD* вредности забележене током симулације молекулске динамике показују да вулканолид испољава високу стабилност протеин-лигандног комплекса у поређењу са андростенолом. Перспективе овог рада су следеће: *in vitro*, *in vivo* и клиничка испитивања за потврђивање рачунарских налаза.

(Примљено 25. новембра, ревидирано 22. децембра 2023, прихваћено 19. фебруара 2024)

REFERENCES

1. R. Tosepu, J. Gunawan, D. S. Effendy, L. O. A. I. Ahmad, H. Lestari, H. Bahar, P. Asfian, *Sci. Total Environ.* **725** (2020) 138436 (http://dx.doi.org/10.1016/J.SCITOTENV.2020.138436)
2. C. Wu, Y. Liu, Y. Yang, P. Zhang, W. Zhong, Y. Wang, Q. Wang, Y. Xu, M. Li, X. Li, M. Zheng, L. Chen, H. Li, *Acta Pharm. Sin., B* **10** (2020) 766 (http://dx.doi.org/10.1016/J.APSB.2020.02.008)
3. A. K. Singh, A. Singh, A. Shaikh, R. Singh, A. Misra, *Diabetes Metab. Syndr. Clin. Res. Rev.* **14** (2020) 241 (http://dx.doi.org/10.1016/J.DSX.2020.03.011)
4. D. Kang, H. Choi, J. H. Kim, J. Choi, *Int. J. Infect. Dis.* **94** (2020) 96 (http://dx.doi.org/10.1016/j.ijid.2020.03.076)
5. P. Zhai, Y. Ding, X. Wu, J. Long, Y. Zhong, Y. Li, *Int. J. Antimicrob. Agents* **55** (2020) 105955 (http://dx.doi.org/10.1016/J.IJANTIMICAG.2020.105955)
6. Y. Shi, J. Wang, Y. Yang, Z. Wang, G. Wang, K. Hashimoto, K. Zhang, H. Liu, *Brain, Behav. Immun. – Heal.* **4** (2020) 100064 (http://dx.doi.org/10.1016/J.BBIH.2020.100064)
7. C. H. Parga-Lozano, *Biomed. J. Sci. Tech. Res.* **35** (2021) 28000 (http://dx.doi.org/10.26717/bjstr.2021.35.005761)

8. Z. Wang, X. Chen, Y. Lu, F. Chen, W. Zhang, *Biosci. Trends* **14** (2020) 64 (http://dx.doi.org/10.5582/BST.2020.01030)
9. A. A. Elfiky, *Life Sci.* **248** (2020) 117477 (https://doi.org/10.1016/J.LFS.2020.117477)
10. B. Robson, *Comput. Biol. Med.* **119** (2020) 103670 (http://dx.doi.org/10.1016/J.COMPBIOMED.2020.103670)
11. V. Pooladanda, S. Thatikonda, C. Godugu, *Life Sci.* **254** (2020) 117765 (http://dx.doi.org/10.1016/J.LFS.2020.117765)
12. R. Hatada, K. Okuwaki, Y. Mochizuki, K. Fukuzawa, Y. Komeiji, Y. Okiyama, S. Tanaka, *J. Chem. Inf. Model.* **60** (2020) 3593 (https://doi.org/10.1021/acs.jcim.0c00283)
13. X. Tang, R. H. Du, R. Wang, T. Z. Cao, L. L. Guan, C. Q. Yang, Q. Zhu, M. Hu, X. Y. Li, Y. Li, L. R. Liang, Z. H. Tong, B. Sun, P. Peng, H. Z. Shi, *Chest* **158** (2020) 195 (http://dx.doi.org/10.1016/j.chest.2020.03.032)
14. J. Fantini, C. Di Scala, H. Chahinian, N. Yahi, *Int. J. Antimicrob. Agents* **55** (2020) 105960 (http://dx.doi.org/10.1016/J.IJANTIMICAG.2020.105960)
15. Z. Sahraei, M. Shabani, S. Shokouhi, A. Saffaei, *Int. J. Antimicrob. Agents* **55** (2020) 105945 (http://dx.doi.org/10.1016/J.IJANTIMICAG.2020.105945)
16. A. C. Tsang, S. Ahmadi, J. Hamilton, J. Gao, G. Virgili, S. G. Coupland, C. C. Gottlieb, *Am. J. Ophthalmol.* **206** (2019) 132 (http://dx.doi.org/10.1016/j.ajo.2019.04.025)
17. P. Gautret, J. C. Lagier, P. Parola, V. T. Hoang, L. Meddeb, M. Mailhe, B. Doudier, J. Courjon, V. Giordanengo, V. E. Vieira, H. Tissot Dupont, S. Honoré, P. Colson, E. Chabrière, B. La Scola, J.-M. Rolain, P. Brouqui, D. Raoult, *Int. J. Antimicrob. Agents* **56** (2020) 105949 (http://dx.doi.org/10.1016/J.IJANTIMICAG.2020.105949)
18. J. B. Radke, J. M. Kingery, J. Maakestad, M. D. Krasowski, *Toxicol. Reports* **6** (2019) 1040 (http://dx.doi.org/10.1016/J.TOXREP.2019.10.006)
19. C. Colalto, *Drug Dev. Res.* **81** (2020) 950 (http://dx.doi.org/10.1002/ddr.21716)
20. E. O. Ojah, *Iberoam. J. Med.* **2** (2020) 322 (http://dx.doi.org/10.53986/ibjm.2020.0056)
21. N. Contreras-Puentes, M. Salas-Moreno, L. Mosquera-Chaverra, L. Córdoba-Tovar, A. Alviz-Amador, *J. Pharm. Pharmacogn. Res.* **10** (2022) 469 (http://dx.doi.org/10.56499/jppres21.1328_10.3.469)
22. P. T. Quy, T. Q. Bui, N. M. Thai, L. N. H. Du, N. T. Triet, T. Van Chen, N. V. Phu, D. T. Quang, D. C. To, N. T. A. Nhung, *Open Chem.* **21** (2023) 20230109 (http://dx.doi.org/10.1515/chem-2023-0109)
23. S. Dev, I. Kaur, *Kragujev. J. Sci.* **42** (2020) 29 (http://dx.doi.org/10.5937/kgjsci2042029d)
24. U. J. Meierhenrich, *Rev. Oenologues Tech. Vitivinic. Oenologiques Mag. Trimest. Inform.* **33** (2006) 19 (https://dialnet.unirioja.es/servlet/articulo?codigo=3556037)
25. V. Meyer, *Détection d'homologies lointaines à faibles identités de séquences : Application aux protéines de la signalisation des dommages de l'ADN*, Université Paris--Diderot – Paris VII, 2007 (https://theses.hal.science/tel-00361212)
26. I. Aanouz, A. Belhassan, K. El-Khatabi, T. Lakhlifi, M. El-ldrissi, M. Bouachrine, *J. Biomol. Struct. Dyn.* **39** (2021) 2971 (http://dx.doi.org/10.1080/07391102.2020.1758790)
27. H. Zaki, A. Belhassan, M. Benlyas, T. Lakhlifi, M. Bouachrine, *J. Biomol. Struct. Dyn.* **39** (2021) 2993 (http://dx.doi.org/10.1080/07391102.2020.1759452)
28. K. Arnold, L. Bordoli, J. Kopp, T. Schwede, *Bioinformatics* **22** (2006) 195 (http://dx.doi.org/10.1093/BIOINFORMATICS/BTI770)
29. A. Belhassan, H. Zaki, A. Aouidate, M. Benlyas, T. Lakhlifi, M. Bouachrine, *Moroccan J. Chem.* **7** (2019) 028 (http://dx.doi.org/10.48317/IMIST.PRSM/MORJCHEM-V7I1.12247)

30. A. Belhassan, S. Chtita, H. Zaki, T. Lakhlifi, M. Bouachrine, *Bioinformation* **16** (2020) 404 (http://dx.doi.org/10.6026/97320630016404)
31. M. Biasini, S. Bienert, A. Waterhouse, K. Arnold, G. Studer, T. Schmidt, F. Kiefer, T. G. Cassarino, M. Bertoni, L. Bordoli, T. Schwede, *Nucleic Acids Res.* **42** (2014) w252 (http://dx.doi.org/10.1093/NAR/GKU340)
32. N. Guex, M. C. Peitsch, T. Schwede, *Electrophoresis* **30** (2009) S162 (http://dx.doi.org/10.1002/ELPS.200900140)
33. H. E. Pence, A. Williams, *J. Chem. Educ.* **87** (2010) 1123 (http://dx.doi.org/10.1021/ED100697W)
34. L. Ahmed, Y. Zhang, E. Block, M. Buehl, M. J. Corr, R. A. Cormanich, S. Gundala, H. Matsunami, D. O'Hagan, M. Ozbil, Y. Pan, S. Sekharan, N. Ten, M. Wang, M. Yang, Q. Zhang, R. Zhang, V. S. Batista, H. Zhuang, *Proc. Natl. Acad. Sci. U. S. A.* **115** (2018) E3950 (https://doi.org/10.1073/pnas.1713026115)
35. O. Trott, A. J. Olson, *J. Comput. Chem.* **31** (2010) 455 (http://dx.doi.org/10.1002/jcc.21334)
36. BIOVIA, Dassault Systèmes, Discovery Studio Visualiser 2019, *San Diego: Dassault Systèmes*, 2019 (https://discover.3ds.com/discovery-studio-visualizer-download)
37. H. M. Berman, J. Westbrook, Z. Feng, G. Gilliland, T. N. Bhat, H. Weissig, I. N. Shindyalov, P. E. Bourne, *Nucleic Acids Res.* **28** (2000) 235 (http://dx.doi.org/10.1093/nar/28.1.235)
38. M. Hakmi, E. M. Bouricha, I. Kandoussi, J. El Harti, A. Ibrahimi, *Bioinformation* **16** (2020) 301 (http://dx.doi.org/10.6026/97320630016301)
39. C. Kutzner, S. Páll, M. Fechner, A. Esztermann, B. L. De Groot, H. Grubmüller, *J. Comput. Chem.* **36** (2015) 1990 (http://dx.doi.org/10.1002/JCC.24030)
40. E. F. Pettersen, T. D. Goddard, C. C. Huang, G. S. Couch, D. M. Greenblatt, E. C. Meng, T. E. Ferrin, *J. Comput. Chem.* **25** (2004) 1605 (http://dx.doi.org/10.1002/jcc.20084)
41. M. Martínez-Cifuentes, B. E. Weiss-López, L. S. Santos, R. Araya-Maturana, *Molecules* **19** (2014) 9354 (http://dx.doi.org/10.3390/MOLECULES19079354)
42. A. Kumar, C. G. Mohan, P. C. Mishra, *J. Mol. Struct. Theochem* **361** (1996) 135 (http://dx.doi.org/10.1016/0166-1280(95)04312-8)
43. K. Raghavachari, *Theor. Chem. Accounts* **103** (2000) 361 (https://doi.org/10.1007/S002149900065)
44. A. D. Becke, *Phys. Rev., A* **38** (1988) 3098 (http://dx.doi.org/https://doi.org/10.1103/PhysRevA.38.3098)
45. Gaussian 09, Revision A.01, Gaussian, Inc., Wallingford, CT, 2009. (https://gaussian.com/g09citation/)
46. Gaussview Rev. 3.09, Windows version, Gaussian Inc., Pittsburgh, PA (https://gaussian.com/508_gvw/)
47. T. Pantsar, A. Poso, *Molecules* **23** (2018) 1899 (http://dx.doi.org/10.3390/molecules23081899)
48. M. Popovic, *Microb. Risk Anal.* **23** (2023) 100250 (http://dx.doi.org/10.1016/j.mran.2023.100250)
49. M. Popovic, *Microb. Risk Anal.* **22** (2022) 100231 (http://dx.doi.org/10.1016/j.mran.2022.100231)
50. X. Du, Y. Li, Y. L. Xia, S. M. Ai, J. Liang, P. Sang, X. L. Ji, S. Q. Liu, *Int. J. Mol. Sci.* **17** (2016) 144 (http://dx.doi.org/10.3390/ijms17020144)
51. P. Gale, *Microb. Risk Anal.* **21** (2022) 100198 (http://dx.doi.org/10.1016/j.mran.2021.100198)

52. T. Maass, G. Ssebyatika, M. Brückner, L. Breckwoldt, T. Krey, A. Mallagaray, T. Peters, M. Frank, R. Creutznacher, *Chem. - A Eur. J.* **28** (2022) e202202614 (http://dx.doi.org/10.1002/chem.202202614).